THE JOURNAL OF PHYSICAL CHEMISTRY C
A JOURNAL OF THE AMERICAN CHEMICAL SOCIETY

pubs.acs.org/JPCC
Article

Exploring the Dynamics of Suzuki–Miyaura Cross-Coupling Reactions via Single-Molecule Fluorescence Microscopy: Catalytic Efficiency from SM-TOF Measurements

Izadora F. Reis and Marcelo H. Gehlen*

Cite This: https://doi.org/10.1021/acs.jpcc.4c07269
Read Online

ABSTRACT: In this study, four Suzuki–Miyaura cross-coupling reactions utilizing palladium as a catalyst at the single-molecule (SM) level are investigated, employing total internal reflection fluorescence microscopy and super-resolved optical imaging. Three dispersion methodologies of the precatalyst Pd(II) are examined. The first one involves direct adsorption of Pd onto ionic sites SiO_2^- of the glass surface. In the second, Pd is complexed with a ligand bound to the silica surface, and in the third, Pd complexation occurs with a ligand bound to the surface of a microzeolite particle used as a reaction template. All three methods use extremely low catalyst densities. Analysis of fluorescence intermittency from localized nanospots yields the catalyst conversion rate or single-molecule turnover frequency (SM-TOF), allowing calculation of the average number of product molecules generated by a single catalytic center over time. A significant enhancement in catalytic efficiency is found in the microzeolite template when compared with Pd adsorbed on a ligand-free silica glass surface. In the microzeolite template, each catalyst center on average forms 95 molecules per minute, while Pd adsorbed on silica glass produces only 29 molecules per minute, both with weak dependency among the four reactions studied. Stochastic simulation of the cross-coupling reaction cycle indicates that the SM-TOF value is proportional to the product of the rate constant of the determining step of the cycle by the probability of the catalyst being in its active Pd(0) state. Under this approximation, the rate constant of the determining step of the Suzuki–Miyaura cross-coupling reaction cycle is calculated for all four reactions studied.

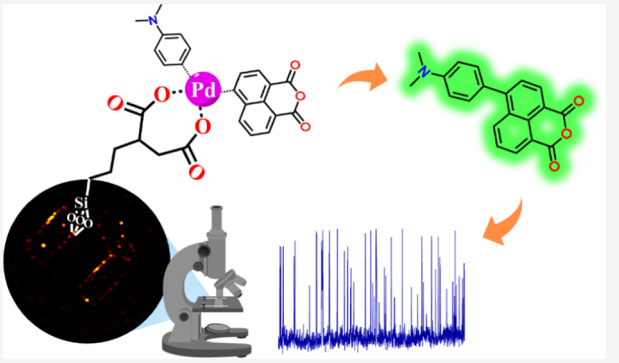

INTRODUCTION

The study of the Suzuki–Miyaura cross-coupling reactions at the single molecule (SM) level is an emerging topic of research.[1−4] For instance, employing high-resolution spatial microscopy in real-time, SM palladium-catalyzed coupling reactions yielding a highly fluorescent dye have been observed. Moreover, aiming to discern whether the reaction takes place on the catalyst surface (heterogeneous process) or is facilitated by the leaching of palladium species into the solution (homogeneous phase) has also been investigated.[5] In recent decades, there have been remarkable advances in the field of fluorescence microscopy with the development of super-resolution and high-sensitivity techniques.[6−10] These techniques have enabled a meticulous assessment of individual systems, providing molecular-level details and precise observation of the photophysics and the chemical and photochemical reactivity on a microscopic scale.[11,12] The application of these advanced fluorescence microscopy techniques is an exceptional opportunity to investigate catalysis in organic reactions such as metal cross-coupling reactions.[13] Nevertheless, other types of techniques with great SM resolution have been applied in the field of molecular reactions.[14] The SM approach becomes very effective when the reaction product or intermediate of the catalytic cycle is a fluorescent species, allowing direct monitoring of emission intensity fluctuations at the catalyst locus.[15,16] It is crucial for obtaining detailed information about reaction kinetics and, therefore, the behavior of the catalyst activity at a molecular scale.[17−19]

Thus, SM reaction experiments under total internal reflection fluorescence (TIRF) detection offer a simple but unique perspective for studying the dynamics of individual molecules and catalysts in real time.[17] This technique, with excitation through evanescent fields, enables the observation of fluorescence from molecules as they are generated in active catalytic sites bound to a glass surface under controlled conditions or using reactive microscopic templates, such as microzeolites.[13,20−23] Zeolites are porous materials widely used

Received: October 25, 2024
Revised: February 4, 2025
Accepted: February 4, 2025

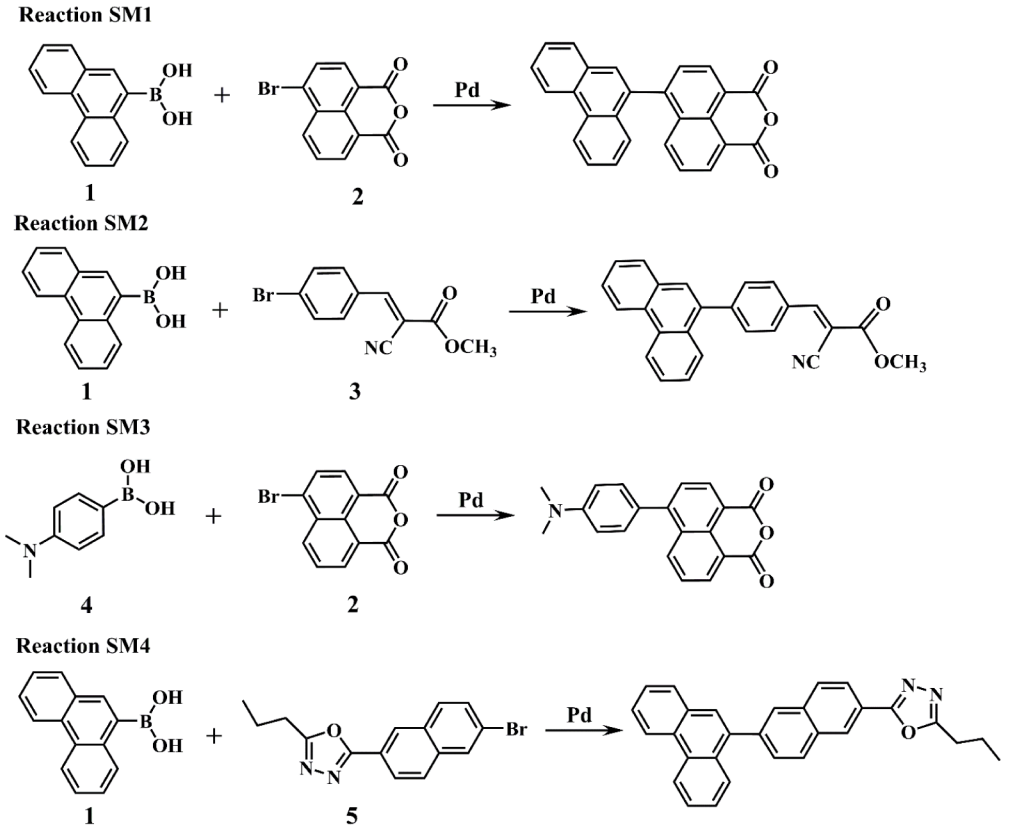

Figure 1. Four reactions explored through the Suzuki−Miyaura cross-coupling reaction in SM experiments are named SM1, SM2, SM3, and SM4. The reagents denoted as 1−5 were as follows: Compound 1: phenanthrene-9-boronic acid; compound 2: 4-bromo-1,8-naphthalic anhydride; compound 3: methyl(E)-3-(4-bromophenyl)-2-cyanoacrylate; compound 4: 4-(dimethylamino)phenylboronic acid; compound 5: 2-(6-bromonaphthalen-2-yl)-5-propyl-1,3,4-oxadiazole.

as catalysts or catalyst supports, composed of crystalline aluminosilicates.[24] The pore size of these zeolites can be adjusted through various modification techniques, enabling selective adsorption and transport of specific molecules.[25]

Additionally, there are acidic sites within these pores that can act as active sites for catalytic reactions.[26] Therefore, due to their highly organized structure and well-defined pore sizes, microzeolites can provide a confined and controlled environment for conducting chemical reactions that would not be possible under conventional conditions.[27,28] Palladium has been immobilized in other solid materials such as thiol-modified mesoporous silica and used as an active catalyst for the Suzuki−Miyaura reaction.[29,30]

In this context, this study presents the results of SM experiments for four Suzuki−Miyaura cross-coupling reactions, forming fluorescent products. The SM kinetic analysis of these reactions was performed employing different methods for Pd catalyst deposition on the glass surface, including the use of silane-functionalized microzeolites as reactive templates. This zeolite L is a micrometer solid particle with an elongated barrel shape, as described and characterized elsewhere.[31,32]

EXPERIMENTAL SECTION

The four reactions under investigation using SM fluorescence experiments are illustrated in Figure 1.

A pivotal aspect of this study involves the exploration of three methods for preparing and depositing Pd(II) precatalyst onto surfaces and the measurement of their catalytic activities at the SM level. In method (I), the precatalyst Pd(II) was adsorbed onto the anionic SiO^- site of the optical glass surface, while in method (II), it was complexed with a silane-bound compound previously deposited on the glass surface using low-pressure vapor deposition, as recently reported.[1,29] In method (III), we expand upon these methodologies by using the Pd(II) complex bound to the surface of cylindrical microzeolites.

The three systems containing Pd (II) precatalyst at low density used for SM experiments are illustrated in Figure 2.

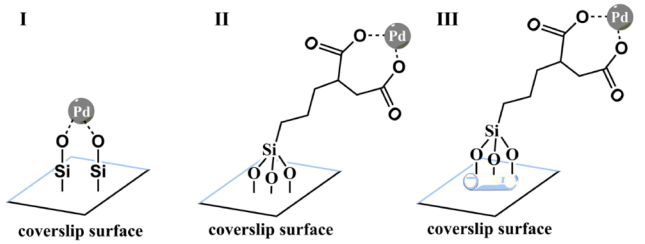

Figure 2. Representation of the three systems containing Pd (II) precatalyst at low density used for SM experiments. (I) Pd adsorbed, (II) Pd complexed, and (III) Pd in labeled microzeolites.

Details of the sample preparation, TIRFM measurements, data treatment of the observed intermittency using the fluctuation threshold method, as well as stochastic simulation of the cross-coupling Pd cycle, are provided in the Supporting Information and elsewhere.[1]

https://doi.org/10.1021/acs.jpcc.4c07269
J. Phys. Chem. C XXXX, XXX, XXX−XXX

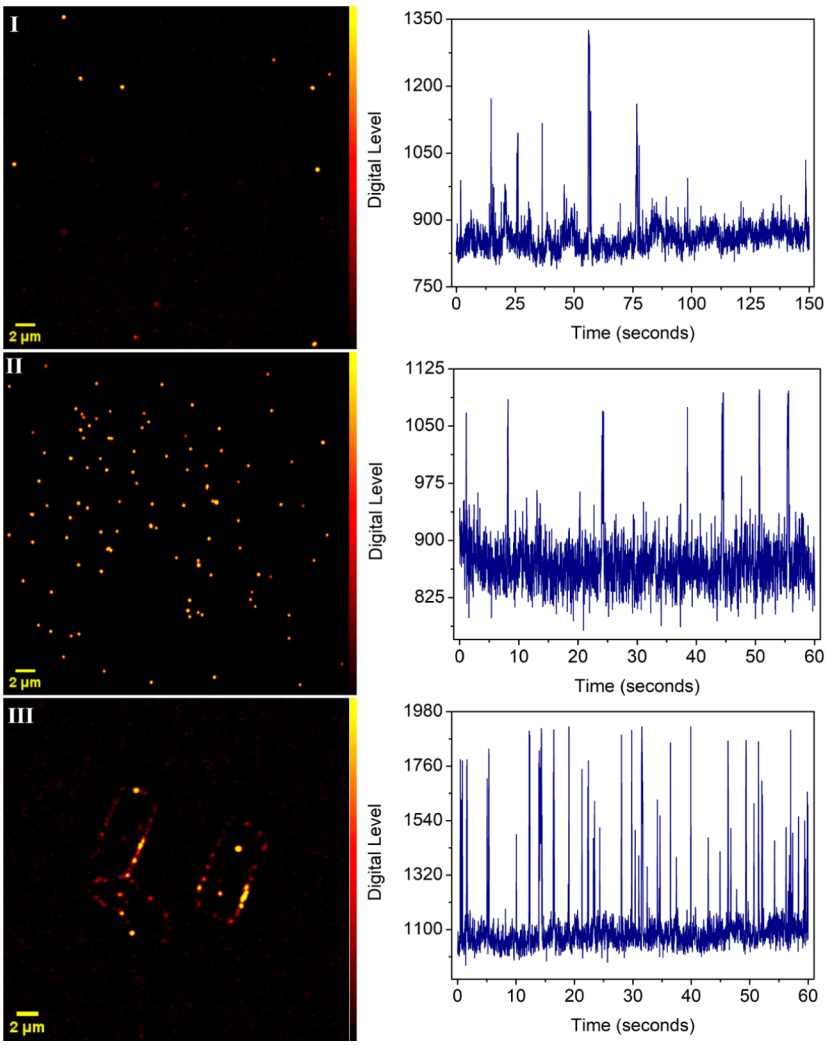

Figure 3. Super-resolved images from SM-TIRFM studies and emission time-trace. (I) Pd adsorbed with 150 s of accumulation time with 20 fps, SM3 reaction; (II) Pd complexed with 80 s of accumulation time with 25 fps, SM3 reaction; and (III) Microzeolites with 60 s of accumulation time with 33.33 fps SM1 reaction. The digital level scale bar represents the summed intensities of the localized molecules. The intermittency of a given nanometric spot is illustrated for each system in the right side of the respective image.

RESULTS AND DISCUSSION

The super-resolution fluorescence images generated by analysis of TIRF movies of the three systems undergoing cross-coupling reactions are illustrated in Figure 3. When the Pd catalyst is dispersed in ionic sites of the glass surface or complexed with a silane diacid ligand, nanoscopic spots with high fluorescence activity appear quite randomly dispersed over a large region (see Figure 3I,II). On the other hand, in microzeolite templates (Figure 3III), the spots with fluorescence activity are concentrated over the external surface of the particle, giving the projection of its cylindrical shape, sometimes forming a dimer or small cluster with particles near each other. Localized fluorescent spots with intermittency behavior are given on the right side of each super-resolution image as typical examples. They are made of discrete fluorescence bursts above the background signal, showing an expected SM intermittency pattern produced by a single catalyst.[33] Statistical analysis of hundreds of fluorescence spots for each system allows the determination of kinetic parameters of the catalytic reaction cycle. In this procedure, the time-trace analysis converts the nonfiltered intensity data of localized fluorescence spots with clear intermittency behavior to a logical on−off (1/0) time series using a fluctuating threshold method.[1] The fluctuating threshold is statistically defined for each point of the time series using a normal distribution, thus converting it to a stochastic logical on−off (1/0) time series. This approach removes the critical assignment of a constant threshold that has been used in many analyses of SM intermittency.

The analysis of the on−off time series allows a direct calculation of several SM parameters of the kinetics, the most important one being the catalyst turnover frequency (SM-TOF) that represents the average SM rate (s^{-1}) of each cross-coupling reaction under the pseudo-first-order approximation because the concentration of reactants used is far higher than the catalyst, and the SM observation is performed over the catalyst turnover cycle. The results of the SM-TOF and other SM parameters for each reaction in the three systems are reported in Table S1. It is worthwhile to mention that the large standard deviation found is a result of the stochastic nature of the reaction process when observed at the SM level.

The corresponding plot of the SM-TOF values as a function of the cross-coupling reaction is given in Figure 4. Although there is a small change in the SM-TOF value with the type of

https://doi.org/10.1021/acs.jpcc.4c07269
J. Phys. Chem. C XXXX, XXX, XXX−XXX

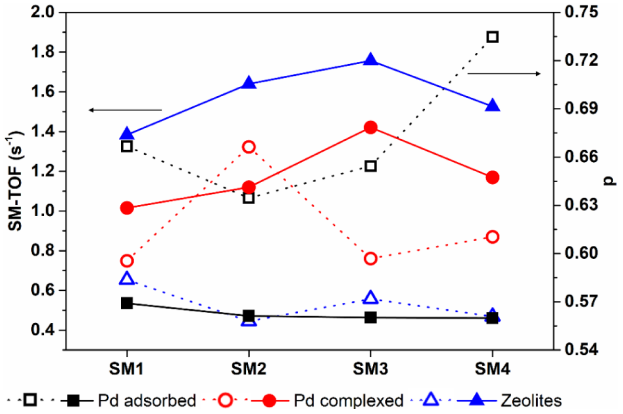

Figure 4. Average SM-TOF (s^{-1}) for the four Suzuki cross-coupling reactions, employing all three functionalization methods and comparative probability of active state (ON) p of the Pd catalyst in the cross-coupling reactions as a function of the Pd dispersion state.

reaction in a given catalytic system, the slightly higher rate observed for reaction SM3 could be ascribed to the substituent effect on compound 4:4-(dimethylamino)phenylboronic acid, where the dimethylamino, as a good electron donor group (EDG), enhances the transmetalation step. However, the most important result is the highest value found in the case of Pd bound to the surface of microzeolites for all reactions studied. On average, it is four times higher than the rate observed in Pd adsorbed onto a ligand-free silica surface. The reason for this high activity observed in microzeolites may be explained by the more exposed Pd catalyst to reactants at first glance. Nevertheless, care should be taken because, on the microzeolite surface, catalyst sites are closer to each other when compared to the two other systems, and, therefore, some cross-talking effect may be present, and the sites could act somewhat cooperatively.

A very interesting point of the statistical analysis of intermittency, performed using the fluctuating threshold method with a Gaussian distribution, is that it enables the estimation of the probability p that the catalyst Pd(0) will be found during the reaction time (the procedure to evaluate p from experimental data is explained in detail in the Supporting Information). The plot of the values of p among the three systems for Pd dispersion is also given in Figure 4. Here, we see an opposite trend to that observed among the values of SM-TOF. Although the Pd adsorbed onto silica anionic sites may have the largest probability of staying in its prompt active form as Pd (0), their measured SM-TOF remains below the corresponding values of the other systems, as already seen in Figure 4. Moreover, it has been pointed out by stochastic simulation of the intermittency of the reaction cycle that SM-TOF = p.k_r, where k_r is the rate-determining constant of the cross-coupling cycle.[1] The stochastic simulation is performed considering the Palladium cross-coupling reaction mechanism (Figure 5a) in its simplified reaction cycle (Figure 5b) with a probability p of finding the active catalyst Pd(0) and a first-order rate constant k_r that represents the determining step that could be ascribed to the oxidative addition of the organic halide in pseudo-first-order or transmetallation (simulation details are found elsewhere).[1]

The linear behavior of SM-TOF = p.k_r is shown in Figure S5 from the analysis of simulated time-trace intensity data and determination of SM-TOF as a function of p and k_r. Assuming

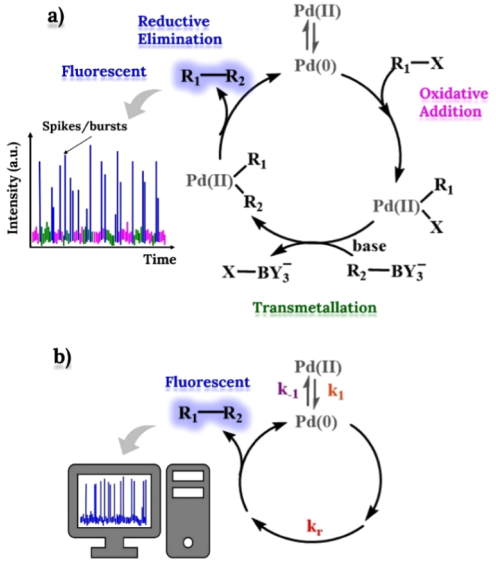

Figure 5. Multistep mechanism of the Pd cross-coupling reaction (a) and its corresponding simplified reaction cycle (b) with a determining step with rate constant k_r used in the stochastic simulation with exponential waiting time distribution. The starting probability of p of active catalyst Pd(0) is given by $p = k_1/(k_1 + k_{-1})$.

that k_r corresponds to the effective SM rate (experimental values are reported in Table S1), k_r is plotted in Figure 6 as a

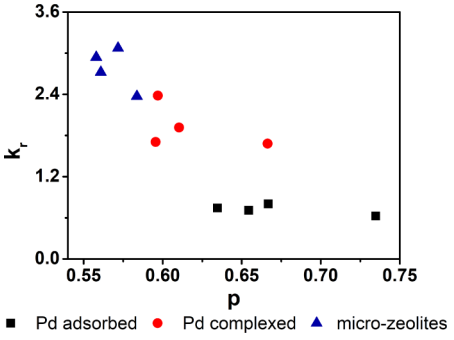

Figure 6. Plot of the intrinsic rate constant k_r (s^{-1}) as a function of the probability p for the four SM reactions in different Pd dispersion state.

function of p. As a result, k_r becomes much more effective in the microzeolite environment, which could indicate that Pd catalyst centers are somewhat acting cooperatively due to their close proximity. As the density of diacid ligands is higher on the microzeolite surface, Pd clustering forming dimers supported on the microzeolite surface may occur and would explain the higher catalyst activity observed.

This effect of high activity has been observed when cross-coupling reactions are performed with a polymer-stabilized Pd catalyst, producing higher TOF values and the formation of Pd nanoparticles after a long reaction time.[34−36] Moreover, the presence of succinic acid groups on the microzeolite surface will provide Pd(0) in close proximity to Pd(II), affording the formation of a dinuclear Pd(I)−Pd(I) dimer, a species considered highly active as a precatalyst.[37] Under these considerations, the ON probability of Pd(0) in microzeolite may be that of having a fraction of dimers as a more active catalytic species stabilized on the template surface. If the Pd(II) reduction forming a dimer is a two-independent step

https://doi.org/10.1021/acs.jpcc.4c07269
J. Phys. Chem. C XXXX, XXX, XXX−XXX

process, then the probability of an active dimer to appear should be seen as p^2 of that of a single Pd in a rough approximation. Thus, using the average of each value of p found (0.57 for microzeolite and 0.70 for Pd adsorbed as a single atom), the relation between microzeolite ON probability with that of single Pd on a glass surface should be given by $0.57 = (0.7)^b$ where b stands for the average size of the Pd(0) cluster formed in microzeolite. Solving the equation above gives b = 1.6, which points out that some degree of Pd clustering is present in the microzeolite templates, explaining its highest activity, as measured by the average SM-TOF values found from intermittency analysis. On the other hand, the effect of catalyst dimer in the SM activity may be simulated considering that its probability of being active is the square of that of a single Pd(0), but the rate constant is larger by a given factor between 2 and 5. The SM fluorescence time trace of stochastic simulation, considering only Pd(0) with a rate constant k_r, is compared with the corresponding data with both Pd(0) and the dimer (with a rate constant $4k_r$) in Figure 7.

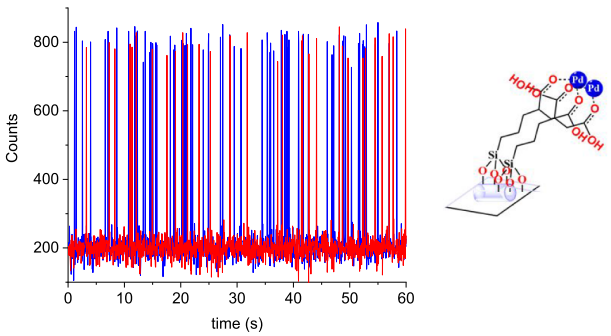

Figure 7. Simulated SM intermittencies of the Suzuki–Miyaura cross-coupling cycle forming a fluorescent product in the condition of only a single Pd(0) catalyst with probability 0.7 and rate constant k_r = 0.6 s^{-1} (red line) and adding a dimer $(Pd)_2(0)$ catalyst with probability 0.5 and rate constant k_r = 2.4 s^{-1} (blue line). The SM-TOF values for each time trace are 0.4 s^{-1} and 1.1 s^{-1}, respectively, corresponding to 24 and 66 product molecules formed per minute in average. Hypothetical dimer stabilized by two neighboring succinic acid groups is given on the right side.

The simulated stochastic intermittencies in the presence of the dimer $(Pd)_2(0)$ resemble the reaction activity observed in microzeolite (see time trace in Figure 4III). Also, the calculated SM-TOF in the presence of the dimer is about three times higher than where only Pd(0) is present, being similar to the ratio of the experimentally observed values of the systems of Pd adsorbed and in microzeolite.

Finally, we have performed experiments with the adsorption of Pd (II) in microzeolite particles free of surface-active succinic acid. The results show that Pd is concentrated in the poles of the microzeolite where the ion exchange process occurs, leading to high catalyst activity, as illustrated in Figure 8. Different from the other system, the local density of Pd is uncontrolled and higher than that of the previous systems, and the intermittency of emission spots in the region departs from the SM behavior.

CONCLUSIONS AND REMARKS

The results obtained in this study point out that the way of loading the Pd catalyst defines the SM-TOF of a given cross-coupling reaction. The use of a microzeolite template with a surface-bound Pd ligand is a more efficient method for achieving higher SM-TOF when compared with Pd adsorbed or complexed with surface sites well dispersed on a flat glass. The highest effectiveness in the microzeolite template system is ascribed to the cooperativity of Pd with more than a single metal complex supported by a succinic diacid ligand in close proximity, acting as an active catalyst.

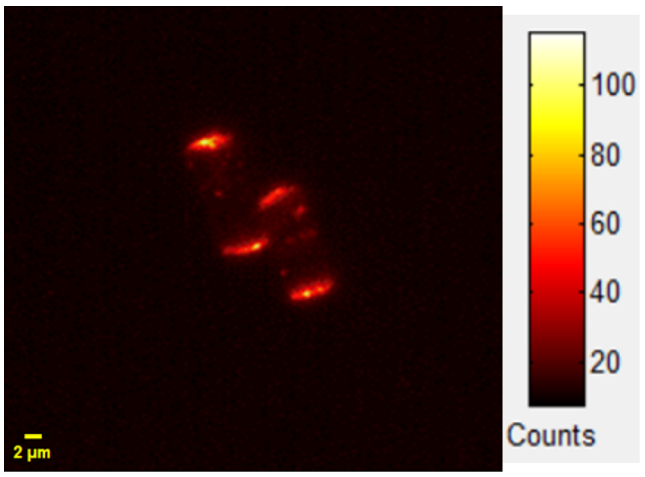

Figure 8. TIRFM image of nonsilanized microzeolite loaded with Pd(II) under reaction SM3. The color scale bar is in relative intensity of photon counts.

ASSOCIATED CONTENT

Supporting Information

The Supporting Information is available free of charge at https://pubs.acs.org/doi/10.1021/acs.jpcc.4c07269.

Method of preparation of microzeolite with Pd; TIRFM measurements; super-resolved images and emission time traces; procedure for the calculation of SM parameters and table of SM rates; analysis of simulated data (PDF)

AUTHOR INFORMATION

Corresponding Author

Marcelo H. Gehlen − *Department of Physical Chemistry, Institute of Chemistry of São Carlos, University of São Paulo, São Carlos 13566-590, Brazil;* orcid.org/0000-0001-9698-8284; Email: marcelog@iqsc.usp.br

Author

Izadora F. Reis − *Department of Physical Chemistry, Institute of Chemistry of São Carlos, University of São Paulo, São Carlos 13566-590, Brazil*

Complete contact information is available at: https://pubs.acs.org/10.1021/acs.jpcc.4c07269

Funding

The Article Processing Charge for the publication of this research was funded by the Coordination for the Improvement of Higher Education Personnel - CAPES (ROR identifier: 00x0ma614).

Notes

The authors declare no competing financial interest.

■ ACKNOWLEDGMENTS

This research was supported by the following Brazilian agencies: São Paulo Research Foundation (FAPESP) grant 2021/01718-9, National Council for Scientific and Technological Development (CNPq) grant 307312/2021-6, INCT-Catalysis/CNPq grant 444061/2018-5, and Coordination of Superior Level Staff Improvement (CAPES) grant 88887.334692/2019-00.

■ REFERENCES

(1) Reis, I. F.; Gehlen, M. H. Single-Molecule Catalysis in the Palladium Cross-Coupling Reaction Cycle. *J. Phys. Chem. Lett.* **2024**, *15*, 2352−2358.
(2) Feng, H.-J.; Sun, X.; Wang, J.-W. A novel COF-based Cu heterogeneous catalyst for a green Suzuki cross-coupling reaction under mild conditions. *New J. Chem.* **2023**, *47* (6), 3104−3111.
(3) Qu, X.; Zhao, B.; Zhang, W.; Zou, J.; Wang, Z.; Zhang, Y.; Niu, L. Single-Molecule Nanocatalysis Reveals the Kinetics of the Synergistic Effect Based on Single-AuAg Bimetal Nanocatalysts. *J. Phys. Chem. Lett.* **2022**, *13* (3), 830−837.
(4) Tachikawa, T.; Majima, T. Single-Molecule, Single-Particle Approaches for Exploring the Structure and Kinetics of Nanocatalysts. *Langmuir* **2012**, *28* (24), 8933−8943.
(5) Costa, P.; Sandrin, D.; Scaiano, J. C. Real-time fluorescence imaging of a heterogeneously catalysed Suzuki−Miyaura reaction. *Nat. Catal.* **2020**, *3* (5), 427−437.
(6) Pelicci, S.; Furia, L.; Pelicci, P. G.; Faretta, M. Correlative Multi-Modal Microscopy: A Novel Pipeline for Optimizing Fluorescence Microscopy Resolutions in Biological Applications. *Cells* **2023**, *12* (3), 354.
(7) Bourgeois, D. Single molecule imaging simulations with advanced fluorophore photophysics. *Commun. Biol.* **2023**, *6* (1), 53.
(8) Mau, A.; Friedl, K.; Leterrier, C.; Bourg, N.; Lévêque-Fort, S. Fast widefield scan provides tunable and uniform illumination optimizing super-resolution microscopy on large fields. *Nat. Commun.* **2021**, *12* (1), 3077.
(9) Gawande, M. B.; Fornasiero, P.; Zbořil, R. Carbon-Based Single-Atom Catalysts for Advanced Applications. *ACS Catal.* **2020**, *10* (3), 2231−2259.
(10) Ouyang, W.; Aristov, A.; Lelek, M.; Hao, X.; Zimmer, C. Deep learning massively accelerates super-resolution localization microscopy. *Nat. Biotechnol.* **2018**, *36* (5), 460−468.
(11) Dedecker, P.; Duwe, S.; Neely, R. K.; Zhang, J. Localizer: Fast, accurate, open-source, and modular software package for super-resolution microscopy. *J. Biomed. Opt.* **2012**, *17* (12), 126008.
(12) Gehlen, M. H.; Foltran, L. S.; Kienle, D. F.; Schwartz, D. K. Single-Molecule Observations Provide Mechanistic Insights into Bimolecular Knoevenagel Amino Catalysis. *J. Phys. Chem. Lett.* **2020**, *11* (22), 9714−9724.
(13) Goldschen-Ohm, M. P.; White, D. S.; Klenchin, V. A.; Chanda, B.; Goldsmith, R. H. Observing Single-Molecule Dynamics at Millimolar Concentrations. *Angew. Chem., Int. Ed.* **2017**, *56* (9), 2399−2402.
(14) Gao, C.; Gao, Q.; Zhao, C.; Huo, Y.; Zhang, Z.; Yang, J.; Jia, C.; Guo, X. Technologies for investigating single-molecule chemical reactions. *Natl. Sci. Rev.* **2024**, *11* (8), nwae236.
(15) An, J.; Song, X.; Wan, W.; Chen, Y.; Si, H.; Duan, H.; Li, L.; Tang, B. Kinetics of the Photoelectron-Transfer Process Characterized by Real-Time Single-Molecule Fluorescence Imaging on Individual Photocatalyst Particles. *ACS Catal.* **2021**, *11* (12), 6872−6882.
(16) Zhang, S.; Fan, D.; Yan, Q.; Lu, Y.; Wu, D.; Fu, B.; Zhao, M. Single-molecule fluorescence imaging of photocatalytic nanomaterials. *J. Mater. Chem. A* **2024**, *12*, 19627.
(17) Saptal, V. B.; Ruta, V.; Bajada, M. A.; Vilé, G. Single-Atom Catalysis In Organic Synthesis. *Angew. Chem., Int. Ed.* **2023**, *62* (34), No. e202219306.
(18) Cordes, T.; Blum, S. A. Opportunities and challenges in single-molecule and single-particle fluorescence microscopy for mechanistic studies of chemical reactions. *Nat. Chem.* **2013**, *5* (12), 993−999.
(19) Bard, A. J.; Fan, F. R. F. Electrochemical detection of single molecules. *Acc. Chem. Res.* **1996**, *29* (12), 572−578.
(20) Fish, K. N. Total internal reflection fluorescence (TIRF) microscopy. *Curr. Protoc.* **2022**, *2* (8), No. e517.
(21) Layek, A.; Van Loon, J.; Roeffaers, M. B. J.; Kubarev, A. V. Correlated super-resolution fluorescence and electron microscopy reveals the catalytically active nanorods within individual H-ZSM-22 zeolite particles. *Catal. Sci. Technol.* **2019**, *9* (17), 4645−4650.
(22) Hendriks, F. C.; Mohammadian, S.; Ristanović, Z.; Kalirai, S.; Meirer, F.; Vogt, E. T. C.; Bruijnincx, P. C. A.; Gerritsen, H. C.; Weckhuysen, B. M. Integrated transmission electron and single-molecule fluorescence microscopy correlates reactivity with ultrastructure in a single catalyst particle. *Angew. Chem., Int. Ed.* **2018**, *57* (1), 257−261.
(23) Lino, A. M.; Gehlen, M. H. Styryl dye formation promoted by catalytic centers of piperazine bound to a silica surface traced by single molecule fluorescence microscopy. *Phys. Chem. Chem. Phys.* **2017**, *19* (31), 20984−20990.
(24) Ruiz, A. Z.; Brühwiler, D.; Ban, T.; Calzaferri, G. Synthesis of Zeolite L. Tuning Size and Morphology. *Monatsh. Chem.* **2005**, *136* (1), 77−89.
(25) Van Loon, J.; Janssen, K. P. F.; Franklin, T.; Kubarev, A. V.; Steele, J. A.; Debroye, E.; Breynaert, E.; Martens, J. A.; Roeffaers, M. B. J. Rationalizing acid zeolite performance on the nanoscale by correlative fluorescence and electron microscopy. *ACS Catal.* **2017**, *7* (8), 5234−5242.
(26) Roeffaers, M. B. J.; De Cremer, G.; Libeert, J.; Ameloot, R.; Dedecker, P.; Bons, A.-J.; Bückins, M.; Martens, J. A.; Sels, B. F.; De Vos, D. E. Super-resolution reactivity mapping of nanostructured catalyst particles. *Angew. Chem., Int. Ed.* **2009**, *48* (49), 9285−9289.
(27) Shen, B.; Wang, H.; Xiong, H.; Chen, X.; Bosch, E. G.; Lazić, I.; Qian, W.; Wei, F. Atomic imaging of zeolite-confined single molecules by electron microscopy. *Nature* **2022**, *607* (7920), 703−707.
(28) Xiong, H.; Wang, H.; Chen, X.; Wei, F. Atomic Imaging of Zeolites and Confined Single Molecules by iDPC-STEM. *ACS Catal.* **2023**, *13* (18), 12213−12226.
(29) Gu, K.; Liu, S.; Liu, C. Surface preparation for single-molecule fluorescence imaging in organic solvents. *Langmuir* **2022**, *38* (50), 15848−15857.
(30) Oleksiievets, N.; Thiele, J. C.; Weber, A.; Gregor, I.; Nevskyi, O.; Isbaner, S.; Tsukanov, R.; Enderlein, J. Wide-Field Fluorescence Lifetime Imaging of Single Molecules. *J. Phys. Chem. A* **2020**, *124* (17), 3494−3500.
(31) Lencione, D.; Gehlen, M. H.; Trujillo, L. N.; Leitão, R. C. F.; Albuquerque, R. Q. (2016) The spatial distribution of the photostability of thionine in zeolite L nanochannels investigated by photobleaching Lifetime Imaging Microscopy. *Photochem. Photobiol. Sci.* **2016**, *15*, 398−404.
(32) Reis, I. F.; Foltran, L. S.; Lauer, M. H.; Gehlen, M. H.; Drekener, R. L.; Correia, C. R. D. Reactive phenanthrene derivatives as markers of amino groups in fluorescence microscopy of surface modified micro-zeolite L. *J. Fluoresc.* **2021**, *31* (5), 1417−1424.
(33) Terentyeva, T. G.; Hofkens, J.; Komatsuzaki, T.; Blank, K.; Li, C.-B. Time-Resolved Single Molecule Fluorescence Spectroscopy of an α-Chymotrypsin Catalyzed Reaction. *J. Phys. Chem. B* **2013**, *117* (5), 1252−1260.
(34) Baran, N. Y. Fabrication and characterization of a novel easy recoverable and reusable Oligoazomethine-Pd(II) catalyst for Suzuki cross-coupling reactions. *J. Mol. Struct.* **2019**, *1176*, 266−274.
(35) Chtchigrovsky, M.; Lin, Y.; Ouchaou, K.; Chaumontet, M.; Robitzer, M.; Quignard, F.; Taran, F. Dramatic Effect of the Gelling Cation on the Catalytic Performances of Alginate-Supported Palladium Nanoparticles for the Suzuki-Miyaura Reaction. *Chem. Mater.* **2012**, *24* (8), 1505−1510.
(36) Borkowski, T.; Zawartka, W.; Pospiech, P.; Mizerska, U.; Trzeciak, A. M.; Cypryk, M.; Tylus, W. Reusable functionalized

https://doi.org/10.1021/acs.jpcc.4c07269
J. Phys. Chem. C XXXX, XXX, XXX−XXX

polysiloxane-supported palladium catalyst for Suzuki-Miyaura cross-coupling. *J. Catal.* **2011**, *282* (2), 270−277.
(37) Fricke, C.; Sperger, T.; Mendel, M.; Schoenebeck, F. Catalysis with Palladium(I) Dimers. *Angew. Chem., Int. Ed.* **2021**, *60*, 3355−3366.

https://doi.org/10.1021/acs.jpcc.4c07269
J. Phys. Chem. C XXXX, XXX, XXX−XXX